

Chapter 12

Wideband Spectrum Sensing

In this chapter, we present an application of compressive sensing to a crucial problem in modern wireless (radio) communication: *How can cognitive radios efficiently identify available spectrum?* We will see that this problem can be cast as one of recovering the support of a sparse signal, in the presence of noise. We will see how the methods and algorithms described in this book will allow us to break theoretical limits of conventional approaches, and once properly implemented in hardware, they can significantly advance the state of the art, by enabling better tradeoffs between energy consumption and scan time.

12.1 Introduction

12.1.1 Wideband Communications

In modern wireless (radio) communication systems, it is common for a wide radio spectrum range to be shared by many users. A classic protocol for sharing a wide spectrum is to divide the spectrum into multiple narrow bands. Each individual user transmits a narrow-band signal within the designated channel band by modulation, typically by multiplying a periodic “carrier signal” with a frequency at the center of the assigned band. To be more precise, let us assume that the entire available spectrum is between

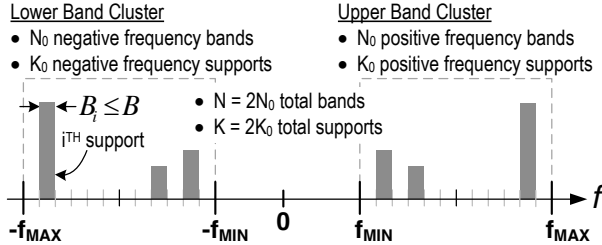


Figure 12.1. A wideband spectrum between (f_{\min}, f_{\max}) (and $(-f_{\max}, -f_{\min})$) is divided into multiple narrow bands of width B . At any given time a (sparse) number of channels are actively in use.

(f_{\min}, f_{\max}) ¹. We denote the bandwidth of the spectrum as $W = f_{\max} - f_{\min}$. If the spectrum is divided into N_0 narrow bands, then each individual channel has a resolution bandwidth (RBW) $B = W/N_0$. See Figure 12.1 for an illustration.

12.1.2 Nyquist Sampling and Beyond

To recover the signals at the receiver side, one needs to demodulate the signal from its carrier, sample the signal at a high frequency through an Analog-to-Digital converter (ADC), and then filter through a low-pass filter. The classic *Nyquist Theorem* [Oppenheim et al., 1999] in digital signal processing stipulates that, to perfectly recover an analog band-limited signal, say $x(t)$, from its discrete (periodic) samples $\{x(nT)\}_{n \in \mathbb{Z}}$, one needs to sample the signal at a frequency $f_s = 1/T$ at least twice as the signal's possible bandwidth, known as the Nyquist rate. Hence in the above wideband setting, if a receiver does not know the carrier frequencies of the (active) channels,² in order to recover the narrow-band signals in every possible channel, one needs to demodulate the signals by sampling at a rate higher than twice the spectrum bandwidth W , that is:

$$f_s \geq 2W.$$

¹For a real signal, its Fourier transform is symmetric in the frequency domain. So for simplicity, we will only talk about the positive (or upper) range of the spectrum (f_{\min}, f_{\max}) , the corresponding negative (lower) spectrum $(-f_{\max}, -f_{\min})$ is assumed to be available too by default.

²which is quite common in many applications such as interference detection. However, if the carrier frequency is known, the receiver can simply demodulate the signals at the carrier frequency [Landau, 1967].

If so, any signal $x(t)$ within this spectrum can be perfectly recovered from its samples $\{x(nT)\}_{n \in \mathbb{Z}}$ via the so called *cardinal series*:

$$x(t) = \sum_{n \in \mathbb{Z}} x(nT) \text{sinc}(t/T - n),$$

or other similar interpolation schemes [Oppenheim et al., 1999].

For wideband communication, however, the Nyquist rate $2W$ often exceeds the specifications of typical analog-to-digital converters (ADC) by magnitudes. For example, in year 2012, the US President's Council of Advisors on Science and Technology (PCAST) recommended sharing 1 GHz of federal government spectrum from 2.7 to 3.7 GHz with nongovernmental entities for public use. The Nyquist rate would require an ADC of 2 GHz! Given that the actual bandwidth B of the signals in each channel is rather small³ compared to the entire spectrum, demodulating at the Nyquist rate for every channel seems rather demanding and likely unnecessary too.

As mobile wireless devices such as cellular phones and personal computers have become ubiquitous in modern day life, it has become increasingly critical to improve the efficiency of spectrum sharing as well as improve the power efficiency of individual mobile devices. In terms of spectrum usage, modern mobile devices are very different from conventional wireless communication systems such as radio broadcasting. At any given time and place, only a relatively small number of devices/users may be active. Hence such devices do not need designated channels at all time and can share a common spectrum via certain data transmission protocols (such as in WiFi). As Figure 12.1 has illustrated, although the PCAST spectrum can simultaneously support N_0 narrow bands, at any given time or place, only a small number of say K_0 bands are active and any new user does not know in advance which bands are being occupied. In such new scenarios, compressive sensing be relevant and beneficial: if the support of a signal is *sparse in the spectrum*, the necessary sampling rate for signal recovery can be significantly lower than the Nyquist rate $2W$. For instance, using techniques such as *random demodulation* [Tropp, 2010], one only needs a sampling rate at

$$f_s = O(K_0 \log(W/K_0))$$

to stably reconstruct the signal, which is exponentially lower than $2W$. A more practical scheme named *modulated wideband converter* [Mishali and Eldar, 2010, Mishali and Eldar, 2011] requires only a sampling rate at

$$f_s = 2K_0B$$

which is usually magnitudes lower than the Nyquist rate when $K_0 \ll N_0$.

³Radios stations are typically assigned a 200 KHz bandwidth. That is more than enough for most audio signals at 20 KHz \sim 30 KHz range. For data transmission tasks of mobile devices, the desired bandwidth is typically 20MHz.

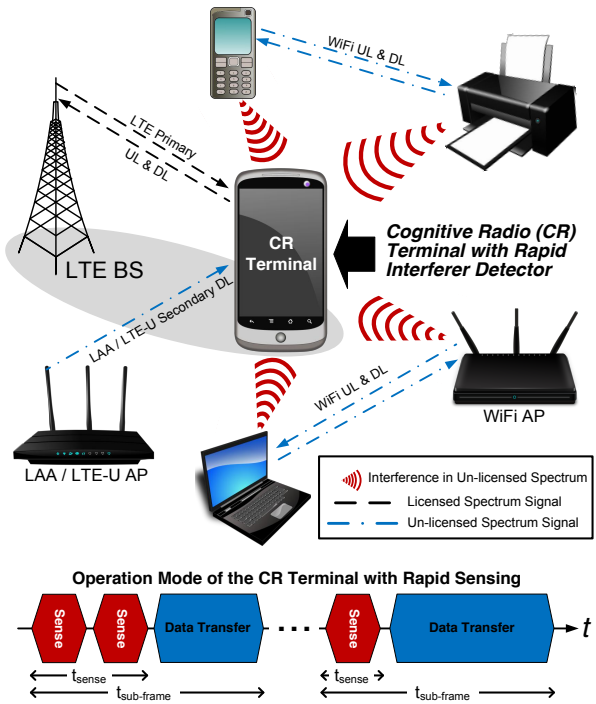


Figure 12.2. Illustration of deployment of LTE-Unlicensed using cognitive ratio (CR) to detect active interferers.

12.2 Wideband Interferer Detection

The next generation 5G technologies like LTE aim to utilize under-utilized unlicensed public spectrum (like the PCAST spectrum mentioned above) in addition to designated licensed spectrum. Figure 12.2 shows an example of such a deployment. In order to utilize and share the unlicensed spectrum efficiently with all other possible users, the user terminal needs to sense in real time which channels have been occupied by other users (called interferers) so that it can opportunistically use other idle channels for subsequence data transfer. Terminals with such capabilities are called cognitive radio (CR) terminals.

To model the interference, we may assume that the entire spectrum (f_{\min}, f_{\max}) are partitioned into N_0 bands. We say a band is occupied (or used) by an interferer (or another user) if the energy on that band is above certain threshold (say above background radio noise level). At any given time, we assume K_0 out of the N_0 bands have been occupied by interferers, as illustrated in Figure 12.3. We call the aggregated signal of all

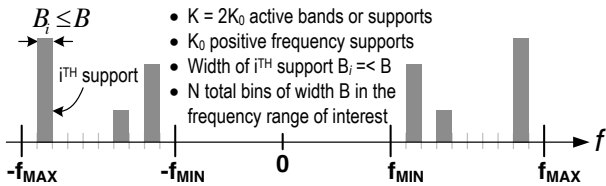


Figure 12.3. At any given time a sparse number of K_0 channels are actively in use.

the interferers as $x(t)$. The problem of interference detection is to find out the supports of the K_0 bands of $X(f)$, the Fourier transform of $x(t)$.

12.2.1 Conventional Scanning Approaches

Conventionally, there are two straightforward approaches to detect (the support of) the interfering signal $x(t)$ in the frequency domain:

1. *Scan one band at a time:* For each of the N_0 bands, one can first down-convert the signal using a local oscillator with frequency f_{lo} at the center of each band

$$f_{lo} = f_{\min} + 0.5B + iB, \quad i = 0, \dots, N_0 - 1,$$

and then sample the signal at the Nyquist rate for each band

$$f_s = 2B.$$

This allows one to recover the component of $x(t)$ in each band and determine if that band has been occupied. Obviously, one needs to repeat this process N_0 times, one for each band, or one can build a system with N_0 parallel branches, again one for each band.

2. *Recover all bands together:* One can first down-convert the signal using a local oscillator with frequency f_{lo} at the center of the entire spectrum

$$f_{lo} = (f_{\min} + f_{\max})/2,$$

and then sample the signal at the Nyquist rate for the entire spectrum

$$f_s = 2W = 2(f_{\max} - f_{\min}).$$

This allows one to recover the entire signal $x(t)$ within the spectrum, regardless which bands have been occupied.

Despite their simplicity, these approaches are costly either in time (e.g. scanning N_0 times), or in hardware complexity (e.g. building N_0 branches), or in energy consumption (e.g. sampling at the high Nyquist rate $2W$).

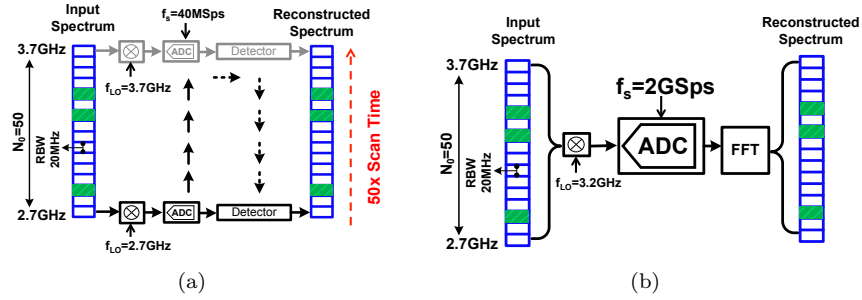


Figure 12.4. Conceptual illustration of the operation of traditional spectrum analysis techniques applied for a 2.7-3.7GHz spectrum analyzer with a 20MHz RBW; the occupied spectrum bins are shaded in green: (a) sweeping spectrum scanner, (b) Nyquist-rate FFT spectrum sensor.

As an example, Figure 12.4 illustrates applying the above schemes to the PCAST spectrum. For a sweeping spectrum scanner (Fig. 12.4(a)), each frequency bin is scanned sequentially by progressively sweeping the local oscillator (LO) driving the downconverter. This architecture requires widely tunable, high quality RF components that are difficult to implement on a chip. Identifying signals over a 1GHz span with a 20MHz RBW requires a long scan time which is proportional to the number of bins $N_0 = 50$. This results in large energy consumption and the risk of missing fast changing interferers.

The scan time in sweeping scanners can in principle be reduced by using a multi-branch architecture with multiple narrowband scanners operating in parallel. However, the hardware complexity becomes impractical since each branch requires a separate phase-locked loop (PLL) to generate the LO signal and the 50 PLL frequencies would need to be spaced closely with a distance equal to the 20MHz RBW.

A Nyquist-rate FFT spectrum sensor (Fig. 12.4(b)) for a 1GHz bandwidth would require a prohibitively high aggregate analog-to-digital (A/D) conversion rate of 2GSps after I/Q downconversion. Even though the scan time is reduced, this is a power hungry approach due to the high sampling rate required for the Nyquist-rate wideband sensing.

How can we do better? As we have mentioned earlier, at any given time, the number of bands used by other users, K_0 , is typically sparse with respect to N_0 . By exploiting this additional knowledge about the spectrum of the interference $x(t)$, i.e., $X(f)$ being sparse, we can come up much more efficient solutions than the above approaches using techniques from compressive sensing. It has been well studied in Chapter 3 that one can recover a sparse signal from a small number of random (incoherent) linear measurements. However, here the sparsity is in the frequency domain and we need to know how to effectively and efficiently take random linear measurements of $X(f)$.

12.2.2 Compressive Sensing in the Frequency Domain

To take a random linear measurement of the spectrum $X(f)$, [Mishali and Eldar, 2010] and [Haque et al., 2015] have suggested a very clever scheme: one can first multiply $x(t)$ with a periodic mixing function $p(t)$ say of period T_p . The mixed signal is then truncated with a low-pass filter $h(t)$ with cutoff frequency $1/(2T_s)$ and then filtered signal is then sampled at rate $f_s = 1/T_s$. The hope is that, for properly chosen mixing function $p(t)$, T_p , and T_s , the (discrete-time) Fourier transform of the output sequence, say $y(n)$, would be precisely random linear measurements of the (sparse) spectrum $X(f)$. Below we give a brief sketch of this scheme.

The mixing function $p(t)$, as a T_p -periodic function, can be written as a Fourier expansion:

$$p(t) = \sum_{l=-\infty}^{\infty} c_l e^{j \frac{2\pi}{T_p} lt}, \quad (12.2.1)$$

where c_l is the Fourier coefficient: $c_l = \frac{1}{T_p} \int_0^{T_p} p(t) e^{-j \frac{2\pi}{T_p} lt} dt$.

After $x(t)$ being mixed with $p(t)$, the Fourier transform of the mixed signal $\tilde{x}(t) = x(t)p(t)$ would be

$$\tilde{X}(f) = \sum_{l=-\infty}^{\infty} c_l X(f - lf_p), \quad (12.2.2)$$

where $f_p = 1/T_p$. Since $X(f)$ is band-limited, the above sum will only have finite terms.

If the subsequent filter $h(t)$ is perfect low-pass filter, only the frequencies in the interval $(-\frac{1}{2}f_s, +\frac{1}{2}f_s)$ will stay in the sequence $y[n]$. Hence, the discrete-time Fourier transform of $y[n]$ has the expression:

$$Y(f) = \sum_{l=-L_0}^{L_0} c_l X(f - lf_p), \quad f \in \left(-\frac{1}{2}f_s, +\frac{1}{2}f_s\right), \quad (12.2.3)$$

where L_0 is large enough to cover the support of $X(f)$.

For simplicity, we may stack all the coefficients c_l into a vector $\mathbf{c} \doteq [c_{L_0}, \dots, c_{-L_0}]^*$ of length $L = 2L_0 + 1$ and $X(f - lf_p)$ into another vector:

$$\mathbf{z}(f) \doteq [X(f - L_0 f_p), \dots, X(f - L_0 f_p)]^*. \quad (12.2.4)$$

The vector $\mathbf{z}(f)$ is sparse if $X(f)$ is. We can write the above expression as

$$Y(f) = \mathbf{c}^* \mathbf{z}(f). \quad (12.2.5)$$

The remaining question is how to properly choose the T_p -periodic mixing function $p(t)$ so that the expression in (12.2.3) would be a sufficiently random (or incoherent) measure of non-zero components in $X(f)$. An easy scheme is to make the values of $p(t)$ in each of its period $(0, T_p)$ be a

pseudo-random bit sequence (PRBS) of length L :

$$p(t) = \alpha_k, \quad k \frac{T_p}{L} \leq t \leq (k+1) \frac{T_p}{L}, \quad 0 \leq k \leq L-1, \quad (12.2.6)$$

where α_k is a random variable taking binary values in $\{-1, +1\}$ of equal probability. For so-chosen $p(t)$, its Fourier coefficients c_l can be computed as

$$c_l = \frac{1}{T_p} \int_0^{\frac{T_p}{L}} \sum_{k=0}^{L-1} \alpha_k e^{-j \frac{2\pi}{T_p} l(t+k \frac{T_p}{L})} dt = \sum_{k=0}^{L-1} \alpha_k e^{-j \frac{2\pi}{L} lk} \frac{1}{T_p} \int_0^{\frac{T_p}{L}} e^{-j \frac{2\pi}{T_p} lt} dt.$$

Let us define the scalar $d_l \doteq \frac{1}{T_p} \int_0^{\frac{T_p}{L}} e^{-j \frac{2\pi}{T_p} lt} dt$ and let \mathbf{D} be the diagonal matrix with d_l on its diagonal. Notice that $\{e^{-j \frac{2\pi}{L} lk}\}$ are exactly the (k, l) -th entry of the discrete Fourier transform matrix \mathbf{F} of size $L \times L$. So we have

$$\mathbf{c}^* = \mathbf{a}^* \mathbf{F} \mathbf{D} \quad (12.2.7)$$

where $\mathbf{a} = [\alpha_0, \alpha_1, \dots, \alpha_{L-1}]^*$ is the sequence of random bits.

Combining the above equation with the measurement equation (12.2.5), we have

$$Y(f) = \mathbf{a}^* \mathbf{F} \mathbf{D} \mathbf{z}(f). \quad (12.2.8)$$

The above equation is obtained from mixing with one signal $p(t)$ from one pseudo random bit sequence \mathbf{a} . To recover the sparse vector $\mathbf{z}(f)$, we can mix the input $x(t)$ with multiple signals $p_i(t), i = 1, \dots, m$, each with an independent pseudo random bit sequence \mathbf{a}_i . We collect all the measurements $Y_i(f)$ into one vector $\mathbf{y}(f) = [Y_1(f), \dots, Y_m(f)]^*$. Then we have

$$\mathbf{y}(f) = \mathbf{A} \mathbf{F} \mathbf{D} \mathbf{z}(f), \quad (12.2.9)$$

where \mathbf{A} is $m \times L$ matrix containing all the independent pseudo random bit sequences \mathbf{a}_i as its rows.

Notice that the diagonal operator \mathbf{D} does not change the sparsity of $\mathbf{z}(f)$ and the DFT matrix \mathbf{F} is unitary. As we have known from the analysis in Chapter 3, the $m \times L$ measurement matrix \mathbf{AF} would be highly incoherent and the so obtained measurements $\mathbf{y}(f)$ would be a set of incoherent measurements of $\mathbf{z}(f)$. As long as m is large enough, say in the order $O(K_0 \log(L/K_0))$, we are guaranteed to correctly recover the sparse vector $\mathbf{z}(f)$ using the ℓ_1 minimization:

$$\min \| \mathbf{z}(f) \|_1 \quad \text{subj. to} \quad \mathbf{y}(f) = \mathbf{A} \mathbf{F} \mathbf{D} \mathbf{z}(f). \quad (12.2.10)$$

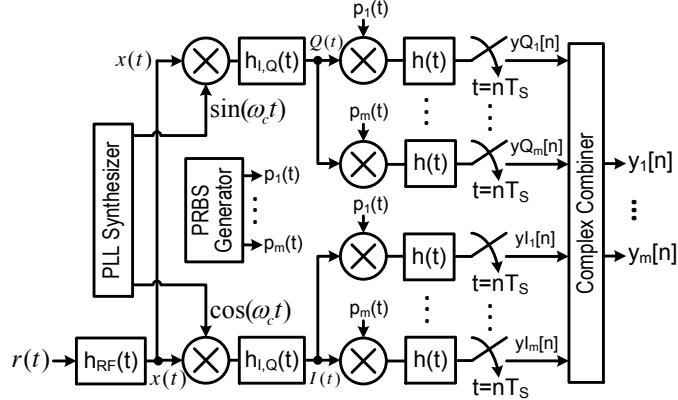


Figure 12.5. System diagram of the Quadrature Analog to Information Converter (QAIC).

12.3 System Implementation and Performance

The remaining issue is how one can implement the above spectrum sensing scheme with a practical real hardware system design? The resulting system should be able to realize the theoretical benefits of compressive sensing and break a good balance between power consumption, scanning time, and hardware complexity. The goal is to achieve significantly improved performance than the conventional approaches mentioned earlier. We here introduce one such system, the so-called Quadrature Analog to Information Converter (QAIC) system [Haque et al., 2015, Yazicigil et al., 2015], for energy-efficient wideband spectrum sensing.

12.3.1 Quadrature Analog to Information Converter

The QAIC illustrated in Figure 12.5 consists of three major functional blocks - an RF downconverter, I and Q path modulator banks (mixers, filters and analog-to-digital converters), and a pairwise complex combiner. The input signal $x(t)$ is first downconverted to complex baseband with the in-phase branch I and the quadrature-phase Q. The downconverter outputs $I(t)$ and $Q(t)$ are multiplied by a periodic pseudo-random bit sequence (PRBS) $p_i(t)$, then filtered and sampled at a low rate in the I and Q path modulator banks. The QAIC exploits the compressive spectrum sensing principles discussed above: multiplication by the PRBS aliases the spectrum such that a portion from each band of the downconverter output signals $I(t)$ and $Q(t)$ appears at a low frequency centered around DC. The outputs of the I and Q path modulator banks are pairwise added by the complex combiner to select either the upper (f_{\min}, f_{\max}) or lower ($-f_{\max}, -f_{\min}$)

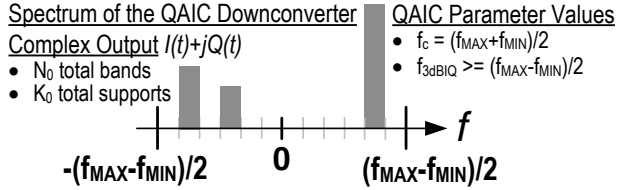


Figure 12.6. QAIC Downconverter Output at Complex Baseband

band cluster of the input signal $x(t)$. The I and Q modulator banks of the QAIC consist of multiple branches each employing a different PRBS such that in principle a sufficiently large number of band mixtures output $y_1[n] \dots y_m[n]$ allows us to recover the sparse multiband signal $x(t)$.

For QAIC, the frequency of the downconverter is chosen to be

$$f_c = (f_{\max} + f_{\min})/2$$

and $\omega_c = 2\pi f_c$. This shifts the spectrum of $x(t)$ from (f_{\min}, f_{\max}) ⁴ to the base range $((-f_{\max} - f_{\min})/2, +(f_{\max} - f_{\min})/2)$, centered around the DC, as shown in Figure 12.6. The low-pass filter $h_{I,Q}(t)$ extracts this base band with a cutoff frequency

$$f_{I,Q} = (f_{\max} - f_{\min})/2.$$

The I and Q path modulator banks employed by the QAIC together process a complex signal $I(t) + j \cdot Q(t)$ at baseband. As a result, the QAIC is able to isolate and process either the upper (f_{\min}, f_{\max}) or the lower $(-f_{\max}, -f_{\min})$ band cluster of the $x(t)$. The spectrum of the QAIC down-converter complex output configured to retain the upper band cluster of $x(t)$ is shown in Figure 12.6.

The span of the QAIC extends from roughly f_{\min} to f_{\max} and QAIC simultaneously observes all bands within this frequency span. Therefore the instantaneous bandwidth of the QAIC is roughly $(f_{\max} - f_{\min})$ Hz, which is partitioned into $N_0 = \lceil (f_{\max} - f_{\min})/B \rceil$ bands with K_0 active bands. With the downconversion, the frequency of the pseudo random bit sequence f_p can be chosen to be

$$f_p = (f_{\max} - f_{\min})/2.$$

Based on the theory of compressive sensing, the number of measurements we need is $m = C_Q K_0 \log(N_0/K_0)$. Due to the quadrature configuration, the total number of branches is then

$$M = 2m = 2C_Q K_0 \log(N_0/K_0),$$

⁴Similar for the lower $(-f_{\max}, -f_{\min})$ band cluster.

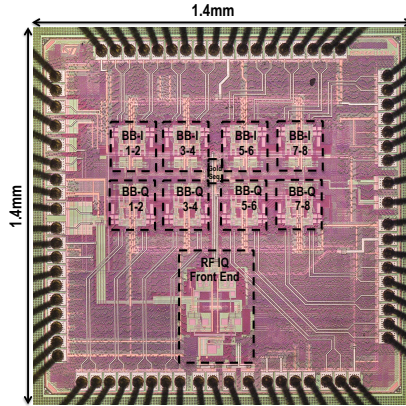


Figure 12.7. Die photograph of the 65nm QAIC prototype

and the output sampling rate (hence the cutoff frequency of the filter $h(t)$ in Figure 12.5) can be half of the band resolution:

$$f_s = B/2.$$

The number of branches M may be traded (say reduced by an integer factor q) for the branch sampling rate f_s (increased by the same factor q).

12.3.2 A Prototype Circuit Implementation

Based on the above design, a first prototype circuit implementation of the QAIC system for detecting up to three interferers in the 2.7–3.7 GHz PCAST spectrum was introduced by [Yazicigil et al., 2015]. The circuit was integrated in a chip implemented with the 65 nm CMOS GP technology, with an active area of 0.428 mm^2 . A photograph of the die of the prototype system is shown in Figure 12.7. We in this section give a brief description of the prototype system.

Figure 12.8 shows the block diagram of the prototype system that employs the QAIC design. The system controller configures the QAIC hardware and software resources according to user specified system constants and performance targets such as RBW, sensitivity, maximum and minimum frequencies of interest, f_{\max} and f_{\min} etc.

The PCAST spectrum is a 1GHz spectrum ranging from 2.7 to 3.7GHz with a RBW of 20MHz. For the QAIC design, $m = 8$ I/Q branches would be sufficient, which is a total of $M = 16$ physical branches. The length of random sequence is chosen to be $L = 63$. More detailed justification of the chosen parameters and other specifications of the system can be found in [Yazicigil et al., 2015].

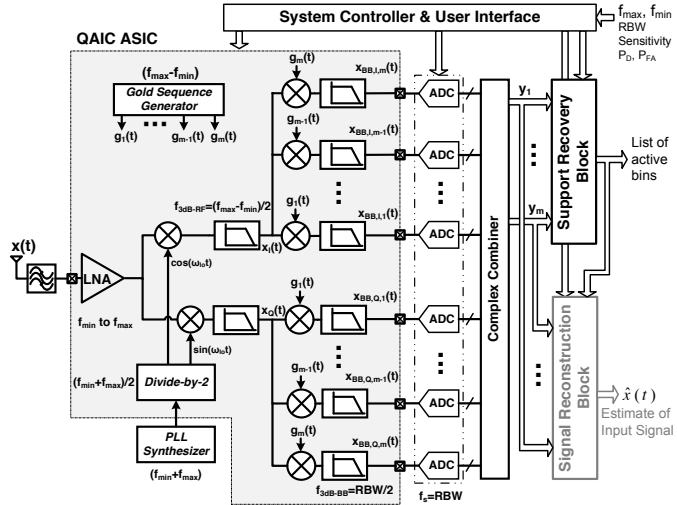


Figure 12.8. Block diagram of the rapid interferer detector based on band pass compressed sampling with a QAIC.

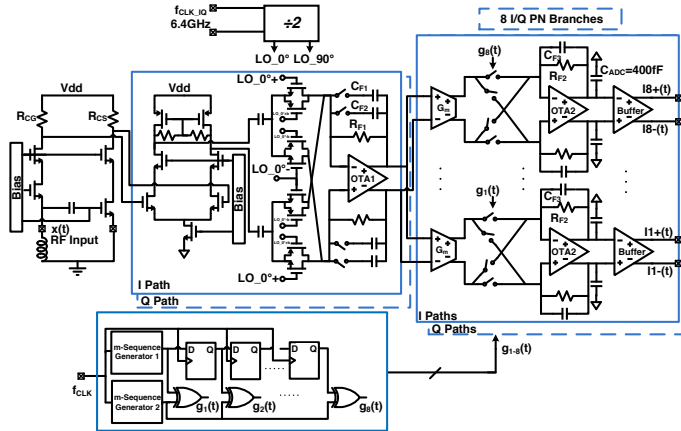


Figure 12.9. Circuit implementation details of the QAIC front end.

Compared to the conventional approaches mentioned in section 12.2.1, the QAIC based spectrum sensor is 50 times faster scan time compared to the sweeping spectrum scanners while 6.3 times compression in the aggregate sampling rate (or in the number of branches) compared to multi-branch spectrum sensors and Nyquist-rate FFT spectrum scanners.

Circuit Implementation of the RF Front-End Blocks

The 2.7-3.7GHz QAIC prototype circuit implementation is shown in Fig. 12.9. It implements the functions in the shaded box in the system diagram in Fig. 12.8. The chip has been implemented in a 65nm CMOS GP technology. The QAIC chip uses a wideband noise-canceling low-noise amplifier (LNA) [Bruccoleri et al., 2004, Blaakmeer et al., 2008]. A wideband noise-canceling LNA is preferred since impedance matching is required for an instantaneous bandwidth of 1GHz. The post-layout simulated LNA gain for typical process corner is 15.8dB to 14.6dB from 2.7 to 3.7GHz and the simulated $S_{11} < -10dB$ for a wide bandwidth from 1 to 3.7GHz for typical process corner. The measured LNA power consumption is 14mW from 1.1V supply.

The LNA is followed by current-driven passive I/Q mixers and transimpedance amplifiers (TIAs) [Mirzaei et al., 2009, Bagheri et al., 2006, Razavi, 1998]. The input stage is implemented as a transconductance G_m amplifier operating at an RF frequency range 2.7 to 3.7GHz followed by four pairs of CMOS transmission gate switches driven by complementary clock phases at 3.2GHz. An off-chip RF clock fed to the chip is 6.4GHz and 3.2GHz quadrature LO signals with a 50% duty cycle driving the RF I/Q downconverter mixers, $\cos(\omega_{lo}t)$ and $\sin(\omega_{lo}t)$, are generated by the on-chip divide-by-2 circuit that is followed by clock buffers and a non overlap generator that is formed by two cross-coupled NAND gates with inverter chains to generate complementary phase clocks for transmission gate type passive mixer switches. The downconverted current signal is converted into a voltage output by a transimpedance amplifier that is configured as an RF I/Q filter. Single stage OTA topology [Razavi, 2001] is chosen for RF I/Q filter design since it was critical to achieve a wide 500MHz bandwidth while driving the 8 I/Q paths and minimizing the power consumption. Measured power consumption of the RF I/Q downconversion stage including the current-driven passive I/Q mixers, TIA based filters and I/Q LO generation based on divide-by-2 circuitry is 20.9mW from 1.1V supply.

PN Sequence Generation and CS Baseband Circuits

The RF TIAs drive eight I/Q paths, each with a current-driven passive mixer and TIA used as a baseband filter loaded with 400fF emulating the equivalent load of an 8-bit ADC (C_{ADC} in Fig. 12.9). Measured power consumption of the 8 I/Q PN branches is 38.9mW from a 1.1V supply.

The I/Q mixing stages are driven by 8 unique gold sequences [Pickholtz et al., 1982, Gold, 1967] generated on-chip with a gold sequence generator. Gold sequences are preferred because a large set of periodic sequences with good cross-correlation and autocorrelation properties can be generated with less circuitry compared to a shift register implementation [Pickholtz et al., 1982]. Gold sequences generated from preferred m-sequence pairs satisfy the following inequalities for cross-correlation, θ [Pickholtz et al., 1982, Gold,

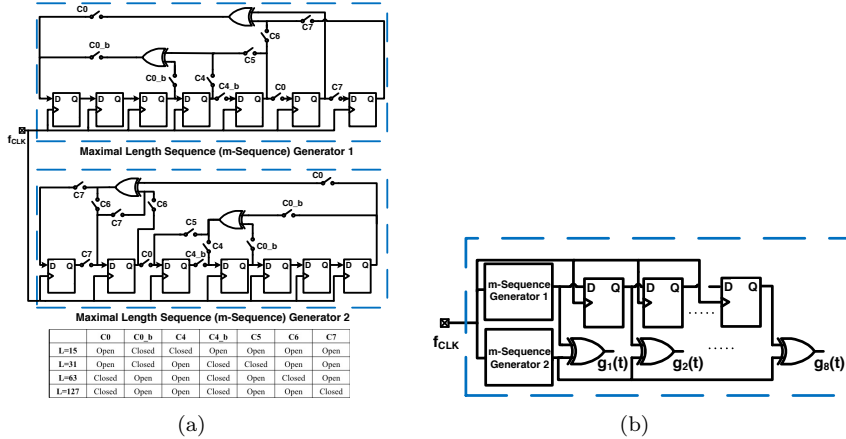


Figure 12.10. Circuit implementation details of gold sequence generator for 8 unique gold sequences with low cross-correlation operating at 1.26GHz for length 15, 31, 63 and 127; (a) Two unique m-sequence generators based on an LFSR implementation (b) 8 unique gold sequences generation based on the two unique m-sequences with RBW programmability.

1967]: $|\theta| \leq t = 2^{(n+2)/2} + 1$, n even and $|\theta| \leq t = 2^{(n+1)/2} + 1$, n odd. The on-chip gold sequence generator (Fig. 12.10) has various length options of 15, 31, 63 and 127 for programmable RBW options and the switches C_0 , C_{0b} , C_4 , C_{4b} , C_5 , C_6 and C_7 are used to control the length of the gold sequences by changing the length of the m-sequences. It generates $8(2^n - 1)$ long gold sequences by XORing two m-sequences generated by two n-flip-flop LFSRs. By keeping one m-sequence (Fig. 12.10(a)) the same and delaying the other one before the XOR, up to $2^n - 1$ distinct gold sequences (Fig. 12.10(b)) can be generated with sufficiently low cross-correlation. Fig. 12.11(a) shows the autocorrelation and cross-correlation properties of one of the 8 unique gold sequences for a length of 63 which satisfy the sequence requirements (i.e. θ). Fig. 12.11(b) shows the measured input referred conversion gain from 2.7 to 3.7GHz of the 8 PN I/Q mixing stages driven by 8 unique gold sequences for a RBW of 20MHz⁵. Measured power consumption of the on-chip gold sequence generator for the nominal length of 63 is 7.04mW from 1.1V supply.

⁵Some of the implemented gold sequences are balanced while others are unbalanced. Balanced gold sequences have better spectral properties (i.e. are more evenly distributed) [Holmes, 2007]. Also 8 unique m-sequences that are known to have uniform (evenly distributed) spectrum can be used in future work to overcome the conversion gain fluctuations over frequency.

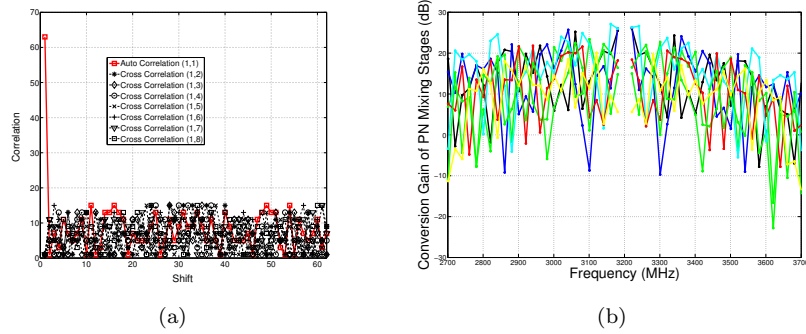


Figure 12.11. Properties of the 8 unique gold sequences generated on chip; (a) Autocorrelation and cross-correlation properties of one of the 8 gold sequences is shown for a shift of 63 for a length 63; (b) Input referred conversion gain from 2.7 to 3.7GHz of the 8 PN mixing stages driven by the 8 gold sequences for a length of 63, and RBW of 20MHz.

CS Digital Signal Processing

The Orthogonal Matching Pursuit (OMP) algorithm is used to identify the input bands that exceed a user-defined threshold. The OMP is a simple greedy heuristic for sparse recovery, which forms an estimate of the signal support one element at a time. It offers an attractive trade-off between algorithm simplicity and recovery guarantees [Tropp and Gilbert, 2007]. The OMP stopping criterion is derived from the system dimension and a user-defined threshold. This threshold can be set to maximize the detection probability P_D or minimize the false alarm probability P_{FA} . In this work, the threshold is set close to the QAIC noise floor to maximize P_D performance of the system.

Overall System Performance

The prototype QAIC system front end is implemented in 65 nm CMOS with a size 0.43 mm^2 and consumes 81 mW from a 1.1 V supply. It can detect up to three interferers in a frequency span of 1 GHz ranging from 2.7 to 3.7 GHz (PCAST Band) with a resolution bandwidth of 20 MHz in $4.4\mu\text{s}$, 50 times faster than traditional sweeping spectrum scanners. Rapid interferer detector with the bandpass QAIC is two orders of magnitude more energy efficient than traditional Nyquist-rate architectures and one order of magnitude more energy efficient than previous low-pass CS methods. The aggregate sampling rate of the QAIC interferer detector is compressed by 6.3 compared to traditional Nyquist-rate architectures for the same instantaneous bandwidth.

12.3.3 Recent Developments in Hardware Implementation

Since the first prototype [Yazicigil et al., 2015], two new chips have been designed to further improve the system's efficiency and compatibility with other communication hardware systems.

Time-segmented QAIC

[Yazicigil et al., 2016] introduced a new chip design that realizes a rapid interferer sensing solution that employs compressed sampling with a time-segmented quadrature analog-to-information converter (TS-QAIC). TS-QAIC enables system scalability by adaptive thresholding in the information recovery engine and by extending the 8 physical I/Q branches of the QAIC to 16 with time segmentation, while limiting the silicon cost and complexity. TS-QAIC can detect up to 6 interferers (compared to 3 for QAIC) over a 1GHz bandwidth between 2.7-3.7GHz in $10.4\mu\text{S}$ with only 8 I/Q physical branches. The TS-QAIC prototype is implemented in 65nm CMOS on a 0.517 mm^2 active area and consumes 81.2mW from a 1.2V supply.

Direct RF-to-Information Converter

The Direct RF-to-information Converter (DRF2IC) [Haque et al., 2017] unifies high sensitivity signal reception, narrowband spectrum sensing, and energy-efficient wideband interferer detection into a fast-reconfigurable and easily scalable architecture. In reception mode, the DRF2IC RF front-end (RFFE) consumes 46.5mW and delivers 40MHz RF bandwidth, 41.5dB conversion gain, 3.6dB NF and -2dBm B1dB. 72dB out-of-channel blocker rejection is achieved in narrowband sensing mode. In compressed sensing wideband interferer detection mode, 66dB operational dynamic range, 40dB instantaneous dynamic range, 1.43GHz instantaneous bandwidth is demonstrated and 6 interferers scattered over 1.26GHz are detected in $1.2\mu\text{S}$ consuming 58.5mW.

12.4 Notes and References

Exercises

12.1 (New Exercise).